Steady state visual evoked potentials-based patient interface under breathing constraints

Xavier Navarro, Sebastien Campion, Fabrizio De Vico Fallani, Pierre Pouget, Thomas Similowski, Mathieu Raux, Mario Chavez

Steady state visual evoked potentials-based patient interface under breathing constraints

X. Navarro*, S. Campion, F. De Vico Fallani, *Member, IEEE*, P. Pouget, T. Similowski, M. Raux and M. Chavez

***Abstract*— Steady state visual evoked potentials (SSVEP) have been widely utilized in brain computer interfacing (BCI) in last years. In this paper, we present a study exploring the possibilities of SSVEP to manage the communication between patients suffering respiratory disorders and health care providers. By imposing different breathing constraints, five healthy subjects communicated their breathing sensations (breathing well/breathing bad) using a visual frequency tagging paradigm: two visual stimuli with different flickering frequencies (15 and 20 Hz) were simultaneously presented on a screen. Using electroencephalographic (EEG) signals from only three EEG electrodes, two spectral features were extracted by a spatial filter in a sliding window, then classified by an unsupervised algorithm based on k-medians. Average detection success rates were of 70% during breathing discomfort, and of 83% when subjects breathed comfortably. Results suggest that SSVEP-based BCI may be a promising choice to improve patient-caregiver communication in situations of breathing discomfort when verbal communication is difficult.**

Keywords: SSVEP, BCI, Spatial filters, k-medians, EEG, mechanical ventilation, patient communication

I. Introduction

Communication problems are common in patients with neuromuscular diseases, paralysis or in semi-consciousness states due to sedative drugs [1]. To facilitate patient-caregiver interaction, steady state visual evoked potentials (SSVEP)-based BCIs are being increasingly employed in clinical environments and rehabilitation. These systems use the physiological property that cortical responses can be modulated by visual-spatial selective attention. Monitoring of SSVEP elicited by multiple flickering stimuli allows a BCI system to detect to which stimulus the subject is attending to. Electroencephalographic signals (EEG) from visual areas are employed to interface the command associated with each stimulus frequency. This technique is easy to implement, it can be applied with no calibration and provides high information transfer rates [2], [3].

EEG is usually processed in short time windows from which spectral features are extracted and then classified. SSVEP frequencies need to be adequately chosen in order perform good classifications. By using a combination of six electrodes, authors in [4] for instance, obtained an average classification accuracy of 84% by selecting the largest test statistic associated to six SSVEP frequencies.

Concerning clinical applications, BCIs using SSVEP have been applied, for instance, to motion disabled persons [7] or in rehabilitation training systems [8]. However, this paradigm has not already been employed to establish a communication pathway with patients receiving mechanical ventilatory assistance or presenting respiratory failure. In this work we address this issue by exploring, for the first time, the potential of a SSVEP brain computer interface to help these patients communicate their breathing discomfort using an automated method. We assess the ability of healthy subjects to communicate their breathing sensations by a SSVEP interface while breathing under several constraints emulating respiratory troubles.

Our paper is organized as follows: In Section II we describe the experimental protocol and the methodology to obtain the features and classify the SSVEPs. Next, Section III shows the performances of the proposed BCI applied online and finally, results are discussed in Section IV.

II. Methods

A. Experimental design

Five healthy subjects (median age = 26 years, interquartile range = 23-30 years) were recruited for this study. They were on a comfortable chair in a dark, isolated room containing a CRT screen monitor placed at 1 m from the subject's head. EEG signals were acquired by three electrodes placed at O1, O2 and Oz positions (plus the ground and reference electrodes at AFz and Cz) according to the 10-20 International System and amplified by BrainAmp hardware (Brain Products, Munich, Germany). Subjects were breathing through a mouthpiece attached to a pneumotachograph (Flow Sensor 279331, Hamilton Medical AG, Rhazuns, Switzerland), a pressure transducer to record respiratory signals. Inspiratory

This work was supported by the program "Investissement d'Avenir ANR-10-AIHU 06" of the French Government and by the grant Legs Poix from the Chancellerie de l'Université de Paris. X. Navarro is supported by Air Liquide Medical Systems through the COVEM project.

X. Navarro is with Sorbonne Universités, UPMC Univ Paris 06, INSERM, UMRS1158, Neurophysiologie Respiratoire Expérimentale et Clinique, Paris, France.

S. Campion and M. Raux are with Sorbonne Universités, UPMC Univ Paris 06, INSERM, UMRS1158, Neurophysiologie Respiratoire Expérimentale et Clinique, Paris, France and with AP-HP, Groupe Hospitalier Pitié Salpêtrière-Charles Foix, Dép. d'Anesthésie-Réanimation, Paris, France.

F. De Vico Fallani is with the INRIA, Paris-Rocquencourt, France and with the CNRS UMR7225 Paris, France and INSERM U1227, UPMC UMRS1127, Institut du Cerveau et de la Moelle Épinière, Paris, France.

P. Pouget and M. Chavez are with the CNRS UMR7225 at the Institut du Cerveau et de la Moelle Épinière, Paris, France.

T. Similowski is with Sorbonne Universités, UPMC Univ Paris 06, INSERM, UMRS1158, Neurophysiologie Respiratoire Expérimentale et Clinique, Paris, France and with AP-HP, Groupe Hospitalier Pitié Salpêtrière-Charles Foix, Service de Pneumologie et Réanimation Médicale, F-75013, Paris, France.

* Corresponding author (e-mail: xavier.navarro@upmc.fr)

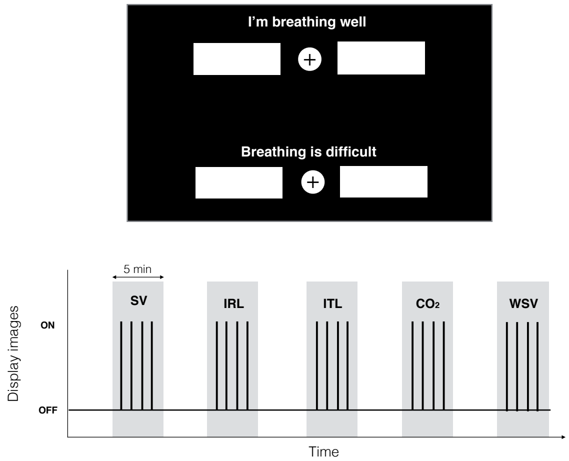

Fig. 1. Top panel: Screen displaying the two images. The upper squares and the circle flickered alternating white/black colors at 15 Hz and the lower ones at 20 Hz. The circle constitutes the focusing point. Bottom panel: Approximate timing of the experiment. Vertical lines constitute the 15-second trials in which the display images appeared (see details in the text).

ventilatory loads were applied to induce ventilatory discomfort in 5-minute sequences as follows:

1) Spontaneous ventilation (SV): subjects breathed comfortably without any constraint.
2) Inspiratory resistive loading (IRL): a resistive load of 50 cm H_2O l^{-1} s^{-1} (7100 Hans Rudolph inc., USA) induced ventilatory discomfort proportional to air flow.
3) Inspiratory threshold loading (ITL): inspiration was conditioned to the production of an inspiratory effort to 50% of maximum inspiratory pressure using a spring-to-stretch device (PowerBreathe Classic, PowerBreath Ltd, UK).
4) Hypercapnia (CO_2): breathing a mixture of 5% CO_2 and 95% O_2 without any mechanical constraint induced metabolic ventilatory discomfort referred to as ”air hunger”.
5) Washout spontaneous ventilation (WSV).

Within each condition, the screen displayed the flickering stimuli only during 15-second trials every minute. At every trial, the subject was asked to focus on a fixed point to ensure that central -and not peripherical- retina was stimulated in all subjects (see Figure 1). Each one of the two images was associated to the labels ”I'm breathing well” and ”Breathing is difficult” oscillating at 15 and 20 Hz, respectively.

Time intervals between respiratory conditions (resting periods) were employed to question the subject about his/her ventilatory comfort during past condition, to modify the experimental set-up and to remind the directions. At the end of each trial the technician questioned the subjects which descriptors of respiratory comfort they had chosen.

B. Pre-processing

Recorded EEG data were firstly down-sampled at 125 Hz (originally sampled at 1000 Hz) and band-pass filtered (a 7th order Butterworth filter, cut-off frequencies $2 - 45$ Hz) to eliminate head movements artifacts and power-line interferences. All algorithms were developed in Matlab language (v7.13.0, MathWorks, USA).

To obtain reasonably fast and reliable detections in real time, the EEG was analyzed in 3-second time windows (with 50% overlap) combining the information from the three referenced, pre-processed channels. Indeed, 3 seconds is a significantly low delay compared to the respiratory dynamics under breathing constraints.

C. Feature extraction

In order to discriminate efficiently a stimulus frequency f and a number of harmonic frequencies N_h, we have used a spatial filter algorithm [4] [9]. Other approaches for SSVEP detection exist, but they use time-locked averaging techniques to reduce the background EEG activity [5] [6]. These methods, however, are not very useful in a BCI setting since they require a large number of trials.

Assuming that visual stimulation with a flicker-frequency of f Hz is applied, we consider $\mathbf{Y}$ as an EEG data segment with N_t samples and N_c channels that can be modeled as a three-component mixing matrix:

$$\mathbf{Y} = \mathbf{XA} + \mathbf{ZB} + \mathbf{E}, \tag{1}$$

with dimension $N_t \times N_c$. Here, $\mathbf{X}$ is the so-called f-model matrix $N_t \times 2N_h$ that contains the real and imaginary components of $e^{j2\pi fht}$ of f and its harmonics, $h = 1 \dots N_h$, with $j = \sqrt{-1}$.

In a similar manner, $\mathbf{Z}$ contains the components relative to both brain activity and external artefacts, also known as nuisance signals. The measurement noise, considered to be stationary within N_t sample windows, is represented by the matrix $\mathbf{E}$. Matrices $\mathbf{A}$ and $\mathbf{B}$ are the corresponding factors scaling the real and imaginary components of $\mathbf{X}$ and $\mathbf{Z}$, respectively.

From the recorded signals $\mathbf{Y}$, we applied a spatial filter to find a combination $\mathbf{S} = \mathbf{ZW}$ such that the nuisance signals are minimized. In our case, since the number of channels is small (N_c=3), we did not reduce the dimension of $\mathbf{S}$, hence $\mathbf{W}$ is a $N_c \times N_c$ matrix containing the weights for each combination in its columns. The minimization problem can be solved by the eigenvalue decomposition of the product $\mathbf{Y_{-f}Y}$, where the first term is obtained as :

$$\mathbf{Y_{-f}} = \mathbf{Y} - \mathbf{X}(\mathbf{X}^T\mathbf{X})^{-1}\mathbf{X}^T\mathbf{Y}, \tag{2}$$

with the sub-index $-f$ denoting the removal of the frequency component f and its N_h harmonics.

The classification features were based on the signal level at the main stimulus frequency f plus the harmonics, and the level of noise when no stimulation is present (between trials). The former could be estimated by the power P_f in the N_h SSVEP harmonic components of $\mathbf{X}^T\mathbf{S}$. To estimate the noise level we require to remove the f component from $\mathbf{S}$:

$$\mathbf{S_{-f}} = \mathbf{Y_{-f}W}, \tag{3}$$

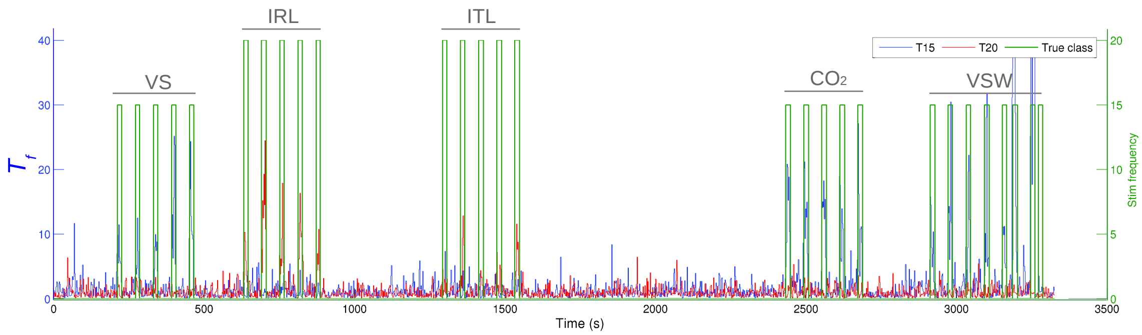

Fig. 2. Values of T_{15} (blue curve) and T_{20} (red curve) during the experiment in subject 3.

Since the noise is underestimated in the above expression [4], the noise power P_{-f} is computed from a 15th order autoregressive model fitted to $\mathbf{S_{-f}}$ (which simulates a baseline noise without stimulus as suggested by [4]). The statistics T_f that reflects the power at frequency f with respect to the no-stimulus power, was obtained by signal-to-noise ratio of the above described estimators, i.e. $T_f = P_f/P_{-f}$. An example of T_f obtained after applying the spatial filters on 15 Hz and 20 Hz can be seen in Figure 2.

D. Classification

The choice of an unsupervised classification algorithm was facilitated by some prior knowledge of the statistics T_{f1} and T_{f2} from the SSVEP frequencies (f_1=15 Hz, f_2=20 Hz). As mentioned before, they correspond to signal-to-noise ratios at each frequency band, so we expected these values to be greater during visual stimulation.

Let θ be an observation vector formed by the pair $[T_{f1}\ T_{f2}]$ at a N_t-sample window and $k = \{0, 1, 2\}$ the three classes labelled according to the frequency viewed by the subject (absence of visual stimuli, f_1 and f_2, respectively). The classical k-means algorithm is a well-known, computationally-effective solution that classifies θ in one of the k groups or clusters by finding the minimal distance to each j-th cluster center:

$$argmin \sum_{j=1}^{k} \sum_{\theta_j} \parallel \theta - \mathbf{c}_j \parallel^2 . \tag{4}$$

The centers $\mathbf{c}_j$ are updated dynamically with the new arrivals by computing the arithmetic mean in the classified observations θ_j:

$$\mathbf{c}_j^{(t+1)} = \frac{1}{t} \sum_{i=1}^{t} \theta_j^{(i)}. \tag{5}$$

Since the mean is more influenced by extreme values than the median, we instead updated $\mathbf{c}_j$ by performing the median value in $\theta_j^{(i)}$, a variant also known as k-medians clustering [10]. Equation 5 can be then rewritten:

$$\mathbf{c}_j^{(t+1)} = median(\theta_j^{(0)}, \theta_j^{(1)}, ..., \theta_j^{(t)}). \tag{6}$$

A known drawback of clustering-based algorithms is that centroids need to be initialized, and a priori information is necessary.

We addressed this issue by simply initializing the centers as follows: $\mathbf{c}_0^{(0)} = [0\ 0]$, $\mathbf{c}_1^{(0)} = [\rho\ 0]$, $\mathbf{c}_2^{(0)} = [0\ \rho]$. Since the presence of visual stimuli implies larger signal-to-noise ratios in classes 1 and 2, then $\rho > 1$. Additionally, we introduced a modification in the k-medians update to increase the control over the sensitivity/specificity pair. A new term and a weight factor is introduced in Eq. (6). Hence, the updating of the centroid is:

$$\widehat{\mathbf{c}}_j^{(t+1)} = (1 - \gamma_j)\theta_j^{(t)} + \gamma_j \mathbf{c}_j^{(t+1)} , \tag{7}$$

where γ_j is an exponential function that depends on the initial conditions and the actual value of the sample :

$$\gamma_j = e^{-\frac{\rho}{\parallel \theta_j^{(t)} \parallel}}. \tag{8}$$

The purpose of introducing a ρ-negative exponential dependency is to penalize new observations having norms lower than ρ, preventing thus the cluster center from moving to the origin, i.e to class 0.

III. RESULTS

We have firstly evaluated the BCI performances as a function of ρ. As it can be observed in Figure 3, lower values provide -on average- higher sensitivity (small values of T_f are classified in 1 or 2 classes due to the proximity to class 0) but at the expenses of a lower specificity. In general, all the performance measures studied evolve almost linearly with respect to ρ, which is a clear advantage of the modified of k-medians over the original algorithm. Indeed, when using a standard k-medians algorithm with $\rho = [1, 2, .., 20]$ to initialize $\mathbf{c}_1^{(0)}$ and $\mathbf{c}_2^{(0)}$ (results not shown here), sensitivities and specificities remained practically unchanged (81/39 % sensitivities and 88/86 % specificities for 15/20 Hz). This is due to the fact that centroids move rapidly to the class median as the number of new observations increase.

On the other hand, to assess the effectiveness of our method in a real implementation, an operating point is fixed by the value of ρ. For $\rho = 20$ for instance, the error rate is minimized at the expenses of lower sensitivity. The choice of $\rho = 20$ corresponds to a trade-off between low false alarm rate and good specificity which is a standard clinical requirement. Other values of ρ (e.g. $\rho = 5$) could provide a

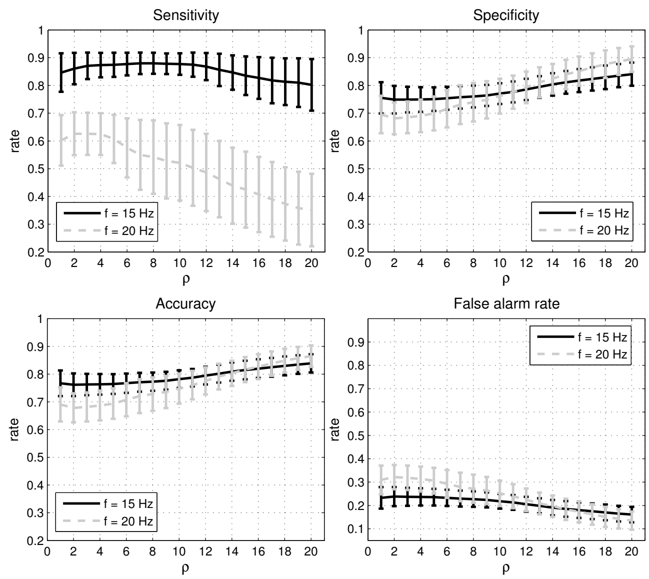

Fig. 3. Performance measures of the proposed method using the modified k-medians classifier. The rates are expressed as the mean $\pm$ standard error measure of the five test subjects.

100% of successful detections, but a much higher false alarm rate.

We have also estimated the success rate, which is a common measure used in BCIs, computed as the number of segments in which there was at least one correct classification over the total number of displaying periods. Such values are reported in Table I for $\rho = 20$.

The poor results observed in subject # 1 might be due to the presence of electromyographic artifacts related to respiratory muscles, or to the subject's distraction during inspiration-constrained tasks. We also notice that some subjects are more receptive to SSVEP at certain frequencies [11]. This issue is currently under study and our results will be presented in a future work.

IV. Conclusion

The present study explored a SSVEP-BCI paradigm as a possible communication pathway under breathing constraints. Results suggest that this technique could be useful to rapidly and automatically identify ventilatory discomfort in healthy subjects to whom ventilation has been artificially impaired.

The proposed approach is fully on-line, calibration free and utilizes only three scalp EEG electrodes and a reference, constituting an easy-to-use alternative in clinical monitoring environments. Although SSVEP detections were less effective during inspiratory constricting tasks than during normal breathing, our preliminary results show that detection of different respiratory states based on respiratory signals underperform those based on EEG (65% and 70-83% respectively).

The performance of detection can be tuned with the parameter ρ. This parameter can be chosen to set low false alarm rates (by increasing ρ), or leave it to 0 to obtain the performances of a classical k-median classifier. In a practical setting, ρ could be fixed in terms of sensitivity/specificity to fulfill a particular clinical requirement (e.g. high sensitivity in critically ill patients).

TABLE I

Results of the BCI performance for the five test subjects employing $\rho = 20$ to reduce false alarm rates.

Subject	#1	#2	#3	#4	#5	Mean
15 Hz % success	93	82	74	93	72	83
20 Hz % success	10	40	100	100	100	70

From the clinical point of view, our approach could be used in intensive care unit patients under mechanical ventilation. Detecting ventilatory discomfort and informing caregivers of its occurrence would lead them to initiate therapeutic actions to restore ventilatory comfort. This technique could also allow the identification of the inspiratory relief produced by an intervention, helping caregivers to ensure they met their objectives.

References

[1] M. B. Happ. Communicating with mechanically ventilated patients: state of the science. *AACN Clinical Issues*, 12(2):247–258, 2001.

[2] G. Bin, X. Gao, Z. Yan, Bo Hong, and S. Gao. An online multi-channel SSVEP-based brain-computer interface using a canonical correlation analysis method. *Journal of Neural Engineering*, 6(4):046002, 2009.

[3] H. Cecotti. Classification of steady-state visual evoked potentials based on the visual stimuli duty cycle. In *2010 3rd International Symposium on Applied Sciences in Biomedical and Communication Technologies (ISABEL)*, pages 1–5, 2010.

[4] O. Friman, I. Volosyak, and A. Graser. Multiple channel detection of steady-state visual evoked potentials for brain-computer interfaces. *IEEE Transactions on Biomedical Engineering*, 54(4):742–750, 2007.

[5] H. Cecotti, A self-paced and calibration-less SSVEP-based brain-computer interface speller *IEEE Transactions Neural Systems and Rehabilitation Engineering*, 18(2): 127–133, 2010.

[6] M. A. Pastor, J. Artieda, J. Arbizu, M. Valencia, and J. C. Masdeu1 Human cerebral activation during steady-state visual-evoked responses *The Journal of Neuroscience 23: 11621-11627, 2003*,

[7] Y. Wang, X. Gao, Bo Hong, Ch. Jia, and S. Gao. Brain-computer interfaces based on visual evoked potentials. *IEEE Engineering in Medicine and Biology Magazine*, 27(5):64–71, 2008.

[8] R. H. Sohn, J. S. Son, H. J. Hwang, C. H. Im, and Y. H. Kim. SSVEP-based functional electrical stimulation system for motor control of patients with spinal cord injury. In C. T. Lim and J. C. H. Goh, editors, *6th World Congress of Biomechanics (WCB 2010). August 1-6, 2010 Singapore*, number 31 in IFMBE Proceedings, pages 655–658. Springer Berlin Heidelberg, 2010.

[9] G. Garcia Molina and V. Mihajlovic. Spatial filters to detect steady-state visual evoked potentials elicited by high frequency stimulation: BCI application. *Biomedizinische Technik/Biomedical Engineering*, 55(3):173–182, 2010.

[10] P. S. Bradley, O. L. Mangasarian, and W. N. Street. Clustering via concave minimization. In *Advances in Neural Information Processing Systems 9*, pages 368–374. MIT Press, 1997.

[11] B. Allison, T. Luth, D. Valbuena, A. Teymourian, I. Volosyak, and A. Graser. BCI demographics: How many (and what kinds of) people can use an SSVEP BCI? *IEEE Transactions on Neural Systems and Rehabilitation Engineering*, 18(2):107–116, 2010.